THE JOURNAL OF BIOLOGICAL CHEMISTRY VOL. 285, NO. 24, pp. 18144–18154, June 11, 2010

Nuclear Export and Centrosome Targeting of the Protein Phosphatase 2A Subunit B56α

ROLE OF B56α IN NUCLEAR EXPORT OF THE CATALYTIC SUBUNIT[*S]

Received for publication, December 8, 2009, and in revised form, April 7, 2010 Published, JBC Papers in Press, April 8, 2010, DOI 10.1074/jbc.M109.093294

Cameron P. Flegg[1], **Manisha Sharma, Cahora Medina-Palazon, Cara Jamieson, Melanie Galea, Mariana G. Brocardo, Kate Mills, and Beric R. Henderson**[2]

From the Westmead Institute for Cancer Research, Westmead Millennium Institute at Westmead Hospital, University of Sydney, Westmead New South Wales 2145, Australia

Protein phosphatase (PP) 2A is a heterotrimeric enzyme regulated by specific subunits. The B56 (or B′/PR61/PPP2R5) class of B-subunits direct PP2A or its substrates to different cellular locations, and the B56α, -β, and -ϵ isoforms are known to localize primarily in the cytoplasm. Here we studied the pathways that regulate B56α subcellular localization. We detected B56α in the cytoplasm and nucleus, and at the nuclear envelope and centrosomes, and show that cytoplasmic localization is dependent on CRM1-mediated nuclear export. The inactivation of CRM1 by leptomycin B or by siRNA knockdown caused nuclear accumulation of ectopic and endogenous B56α. Conversely, CRM1 overexpression shifted B56α to the cytoplasm. We identified a functional nuclear export signal at the C terminus (NES; amino acids 451–469), and site-directed mutagenesis of the NES (L461A) caused nuclear retention of full-length B56α. Active NESs were identified at similar positions in the cytoplasmic B56-β and ϵ isoforms, but not in the nuclear-localized B56-δ or γ isoforms. The transient expression of B56α induced nuclear export of the PP2A catalytic (C) subunit, and this was blocked by the L461A NES mutation. In addition, B56α co-located with the PP2A active (A) subunit at centrosomes, and its centrosome targeting involved sequences that bind to the A-subunit. Fluorescence Recovery after Photobleaching (FRAP) assays revealed dynamic and immobile pools of B56α-GFP, which was rapidly exported from the nucleus and subject to retention at centrosomes. We propose that B56α can act as a PP2A C-subunit chaperone and regulates PP2A activity at diverse subcellular locations.

Reversible protein phosphorylation is a key mechanism regulating a myriad of cellular processes. A delicate balance between the opposing effects of protein kinases and phosphatases determines the functional state of many proteins. Protein phosphatase 2A (PP2A)[3] refers to a major family of heterotrimeric serine-threonine phosphatase enzymes in the cell (1–3). The core enzyme is a dimer consisting of a 36-kDa catalytic C-subunit and a 65-kDa structural regulatory A-subunit, which acts as a scaffold to bring into proximity the C-subunit and protein substrates bound by the diverse regulatory B-subunits. There are four B-subunit gene families each with multiple genes that encode a range of splice variant peptides. The diverse nature of PP2A is inherent in its composition, which is potentially comprised of over 200 distinct protein complexes each containing different combinations of the A-, B-, and C-subunits, and hence allowing for variability and subtle regulation in phosphatase action (3).

The B-subunits are postulated to regulate PP2A activity in different ways: (*a*) by targeting the holoenzyme to specific subcellular locations (*e.g.* B55α directs PP2A to microtubules (4)), (*b*) determining substrate specificity (*e.g.* PP2A complexes containing B55 or B72 B-subunits cause the activation or inhibition of SV40 DNA replication, respectively, because of differences in substrate recognition sites on the SV40 large T antigen (5, 6), and (*c*) by affecting the timing and tissue specificity of phosphatase activity because of differences in their expression.

In contrast to the A- and C-subunits, which are each encoded by two tightly related families, the B-subunits derive from four disparate families that lack any sequence similarity. These gene families are known as the B/PR55, B′/PR61/B56 (hitherto referred to as the B56 family), B″/PR72 and B′ ″/PR93/PR110 families (reviewed in Refs. 1, 2). Five primary members of the B56 family (α, β, γ, δ, and ϵ) have been identified to date, and are encoded by distinct genes. B56 subunits share a highly conserved central region of 80% identity (which comprise two A-subunit binding domains), with variable N- and C-terminal regions postulated to direct the subcellular localization and substrate binding specificity of these proteins. It was proposed that B56α, B56β, and B56ϵ target PP2A activity to the cytoplasm, whereas B56δ and B56γ3 target it to the nucleus (7, 8). Surprisingly, after more than a decade the intracellular targeting mechanisms responsible for nuclear and cytoplasmic positioning of the B56 subunits have not yet been defined.

* This work was supported by the National Health and Medical Research Council of Australia (NHMRC) and the Australian Research Council.

[S] The on-line version of this article (available at http://www.jbc.org) contains supplemental Figs. S1–S6.

[1] Present address: School of Medical Science, Griffith University Gold Coast Campus, Queensland 4215, Australia.

[2] An NHMRC Senior Research Fellow. To whom correspondence should be addressed: Westmead Millennium Institute, Darcy Road (P.O. Box 412), Westmead, NSW 2145, Australia. Tel.: 61-2-9845-9057; Fax: 61-2-9845-9102; E-mail: beric_henderson@sydney.edu.au.

[3] The abbreviations used are: PP2A, protein phosphatase 2A; APC, adenomatous polyposis coli; FRAP, fluorescence recovery after photobleaching; GFP, green fluorescent protein; NLS, nuclear localization signal; NES, nuclear export sequence; PBS, phosphate-buffered saline; YFP, yellow fluorescent protein; HA, hemagglutinin; LMB, Leptomycin B; mAb, monoclonal antibody.

The PP2A B56 subunits play integral roles in cancer, through their regulation of c-Myc protein stability and expression (9), Bcl-2 phosphorylation (10), and the Wnt signaling pathway (11–14). The key mediator of the Wnt signaling pathway is the multifunctional protein β-catenin, which when overexpressed causes transactivation of genes that directly promote cell transformation and cancer. B56α has been shown to bind proteins that regulate β-catenin stability, including APC (11, 15) and p63 (13). The B56β and B56γ subunits bind to axin (16), which is also a key component of the β-catenin and c-Myc degradation complexes. B56α has been shown to negatively regulate the Wnt signaling pathway by reducing β-catenin levels and inhibiting the transcription of β-catenin target genes through an APC-dependent mechanism (11, 12, 16).

We previously reported that B56α binds to the first four repeats of the Armadillo repeat domain of APC and promotes its nuclear accumulation (15). Given that B56α is also a key component of the β-catenin degradation complex, a more complete understanding of its subcellular location is important for understanding its functional roles. Therefore, in this study we used a range of biochemical and cell assays to detect B56α and characterize its nuclear transport and centrosomal localization in fixed cells and live cells. Its cytoplasmic distribution was regulated by nuclear export, and we identify a functional nuclear export sequence (NES) in the C terminus of B56α, and show that this sequence in conserved only in those B56 subunits (β and ϵ) known to locate predominantly to the cytoplasm. Functional implications including a role for B56α in nuclear export of the PP2A C-subunit are discussed.

MATERIALS AND METHODS

Cell Lines and Transfection—NIH 3T3 fibroblast cells, U2OS osteosarcoma epithelial cells, HeLa cervical carcinoma cells, and T47D breast carcinoma cells were cultured in Dulbecco's modified Eagle's medium with 10% fetal calf serum and were free of mycoplasma. NIH 3T3 and U2OS were the main cell lines used to test nuclear export of endogenous and ectopic B56α. HeLa cells were used for centrosome analysis as they displayed the clearest B56α-GFP staining in live cells for photobleaching assays. T47D is our cell line of choice for the Rev(1.4)-GFP-based nuclear export assay (see below). Leptomycin B (LMB) (Sigma) was added to a final concentration of 6 ng/ml. Human CRM1 siRNA pool was purchased from Santa Cruz Biotechnologies and used at 2 μg/ml. DNA transfection of cells (typically 1 μg of DNA per 2 ml of medium) was performed with FuGene reagent as directed (Roche), using cells at medium density seeded onto coverslips. Some transfections were performed with Lipofectamine reagent (Invitrogen).

Plasmid Construction—The plasmid pB56α-GFP was constructed by cloning the full-length B56α cDNA sequence from pHA-B56α (provided by D. Virshup, University of Utah) into the vector pEGFP-N1 (Clontech). The B56 coding sequence (amino acids 1–486) was amplified by PCR using forward (5′-TTACTCGAGTTCGCCACCATGTCGTCGTCGTCG-3′) and reverse (5′-ATATGGATCCTTTTCGGCACTTGTA-TTGCT-3′) primers containing Xho1 and BamH1 restriction sites, respectively. The sequences was then inserted upstream of GFP in the pEGFP-N1 vector. Subfragments of the B56α sequence were cloned using the same strategy into pEGFP-N1. The plasmid pYFP-CRM1 was described previously (17). The nuclear export assay test sequences were amplified by PCR from the B56α cDNA template (or from overlapping oligonucleotides corresponding to sequences from B56β and ϵ) and cloned into the BamH1/Age1 sites of pRev(1.4)-GFP as described in detail in Henderson and Eleftheriou (18). The full-length NES mutant form of B56, pB56α(L461A), was created by PCR-amplifying a B56α sequence containing the L461A mutation and using this to replace the wild-type sequence between Xba1 and HindIII sites in pB56α-GFP. All constructs were confirmed by sequencing.

Cell Fractionation and Western Blot—NIH 3T3 and U2OS cells were separated into nuclear and cytoplasmic fractions using the NE-PER kit (Pierce) as directed. Equivalent proportions of each cell fraction (60 μg of cytoplasm, 20 μg of nuclear extract) were separated on 8% SDS-polyacrylamide gels and transferred to Immobilon-P membranes (Millipore). Filters were blocked with 3% bovine serum albumin/PBS for 1 h and probed with the following primary antibodies: B56α mouse monoclonal antibody (1:1000, Becton Dickinson), PP2A C-subunit polyclonal antibody (1:1000, Cellular Signaling), PP2A A-subunit polyclonal antibody (1:1000 Cellular Signaling), CRM1 polyclonal antibody (H300, Santa Cruz Biotechnologies) and topoisomerase II antibody Ab1 (Santa Cruz Biotechnologies) as a fractionation control at room temperature for 2 h, followed by incubation with horseradish peroxidase-conjugated secondary antibody (1:5000; Sigma) for 1 h at room temperature. B56α and PP2A C-subunit were detected at the expected sizes (endogenous B56α at 56 kDa; ectopic B56α-GFP at ~83 kDa; endogenous PP2A C-subunit at 36 kDa) as confirmed by size markers. Filters were developed with an ECL chemiluminescence reagent (Amersham Biosciences) exposed to x-ray film and quantitated by densitometry.

Transfection and Immunofluorescence Microscopy—Cells grown on coverslips in a 6-well dish (Nunc) and 12-h post-seeding were transfected with 2 μg of plasmid using Fugene-6 (Roche). The lipid-DNA mix was left on cells for 5 h before replacing the medium and processing 30 h later. Cells were fixed with 3.7% formalin/PBS for 20 min at room temperature or chilled methanol/acetone for 5 min on ice, depending on the cellular compartment to be analyzed. Cells were either directly mounted for detection of GFP fluorescence or blocked with 3% bovine serum albumin and stained with primary antibodies: anti-pericentrin (1:2000 dilution, polyclonal antisera from Abcam) to detect the centrosome, anti-nucleoporin antibody at (1:1200 dilution of mAb414, Covance) to detect the nuclear envelope, treatment with the Mitotracker Red dye CMX-ROS (Molecular Probes) to detect the mitochondria, anti-α-tubulin mAb (A-11126, 1:200, Molecular Probes) to detect microtubules, and polyclonal antisera against human PP2A A- and C-subunits (Cellular Signaling), and then washed three times with PBS. Cells were subsequently incubated with anti-mouse Alexafluor-488 or Alexafluor-594 (Invitrogen) at 1:1500 dilution at room temperature. After extensive washes in PBS, cells were mounted with Vectashield (Vector Labs) and visualized by microscopy. Cells were photographed with an Olympus fluorescence microscope at ×400 magnification, or

digital images were captured using an Olympus FV1000 confocal microscope at ×600 magnification. For z-stacks (*e.g.* nuclear rim), 12 images were taken at 0.3 μM step size.

Confocal Microscopy and Photobleaching (FRAP) Assays—Subconfluent HeLa cells were transfected with B56α-GFP using Fugene-6 and after 30 h were subjected to FRAP (fluorescence recovery after photobleaching) analysis using an Olympus FV1000 confocal microscope. Transfected cells were selected and for nuclear export kinetics, >90% of the cytoplasm was bleached using 100% laser power, after which fluorescence recovery was monitored over a period of 360 s. For nuclear import, a similar analysis was performed after bleaching of the nuclear B56α-GFP fluorescence (see Ref. 19 for more details). The mean recovery curve for B56α was plotted against time. The fluorescence intensity was calculated as the cytoplasmic to nuclear ratio (for export) or nuclear to cytoplasmic ratio (for import) which was preset to 100% based on pre-bleach values. The recovery was measured at 0.5-s intervals for the first 32 s, then subsequently at 1-s intervals for the next 30 s and then at 10-s intervals for another 300 s. Cd-tomato (~60kDa) protein was used as a negative control. Each type of FRAP analysis was based on at least 8 cells. For FRAP analysis of centrosome recovery, HeLa cells were co-transfected with B56α-GFP and pericentrin-RFP (gift from Dr. Sean Munro, see Ref. 20). Pericentrin-RFP was used to mark the centrosome in live cells. B56α-GFP at the centrosome was spot-bleached for 1.5 s with 100% laser power and recovery fluorescence was imaged at 1-s intervals over a 160-s period. Similar spot-bleach analysis was done in adjacent cytosolic regions over 100 s.

Rev Nuclear Export Assay—The assay used to assess nuclear export activity was described previously in detail (18). The assay is based on scoring the cellular distribution of GFP fusion proteins expressed following transfection into T47D breast cancer cells. The reference vector, pRev(1.4)-GFP, contains an export-deficient form of Rev-GFP which retains a nuclear localization signal and therefore accumulates in the nucleus/nucleolus of cells. The ability to block nuclear import (with actinomycin D) or export (with leptomycin B) allows for comparison of the export activity of test NESs inserted into the control vector.

RESULTS

B56α Shuttles between Nucleus and Cytoplasm—Previous studies found that HA-tagged B56α was predominantly cytoplasmic and excluded from the nucleus of transfected cells (7, 8). This contrasts with the nuclear staining observed for the B56-γ1 and B56-δ isoforms (7, 8). We compared the localization patterns of HA-B56α and GFP-tagged B56α in transfected NIH3T3 and U2OS cells and observed both nuclear-cytoplasmic and exclusive cytoplasmic staining patterns (Fig. 1*A* and data not shown). Currently there are no specific antibodies for detection of endogenous B56α by immunofluorescence microscopy.

The presence of B56α in both nucleus and cytoplasm raised the possibility that the protein shuttles between the two compartments. In order to test this, the subcellular localization of transiently expressed B56α-GFP was scored in NIH 3T3 cells and U2OS cells in the presence or absence of leptomycin B (LMB, a CRM1-specific nuclear export inhibitor) treatment. In both cell lines, when export was blocked by LMB, B56α displayed a significant shift to the nucleus (Fig. 1*A*). LMB did not cause a complete re-localization of B56α due to some cytoplasmic retention of the protein. We then compared the subcellular distribution of endogenous B56α by cell fractionation and Western blot analysis. In untreated NIH 3T3 cells the B56α was predominantly cytoplasmic, however its distribution shifted significantly (~35%) to the nucleus after 3 h of LMB treatment (Fig. 1*B*). In addition to drug treatment, we knocked down CRM1 expression by siRNA in U2OS cells (Fig. 1*C*, Western blot, *left panel*) and observed that reduction in CRM1 expression elicited an increase in nuclear staining of B56α-GFP in transfected cells (Fig. 1*C*). These results demonstrate that B56α can exit the nucleus via the CRM1 export pathway.

B56α Nuclear Export Is Stimulated by CRM1 and the Rate of Export Is Faster than Import—The cytoplasmic localization of proteins with NES can be induced by co-expressing the CRM1 export receptor (17, 18). We therefore co-expressed HA-tagged B56α with YFP alone or YFP-CRM1 and scored the subcellular distribution by fluorescence microscopy (Fig. 2, *A* and *B*). When transfected alone, or with the YFP vector, B56α localized roughly equivalently between nucleus and cytoplasm (71–80% nuclear and cytoplasmic staining) in NIH 3T3 cells (Fig. 2*B*). However, after co-expression of YFP-CRM1, B56α shifted significantly to the cytoplasm, with 53% of cells displaying B56α exclusively in the cytoplasm. These results confirm that B56α is regulated by CRM1.

The shuttling activity of B56α indicated that it might transiently accrue at the nuclear envelope. We therefore transfected NIH 3T3 and HeLa cells with B56α-GFP and co-stained with antibodies against CRM1 or the nuclear pore complex, respectively, and analyzed cells by confocal microscopy. The B56α was found to frequently co-localize with CRM1 and nucleoporins at the nuclear envelope, and the B56 nuclear rim pattern extended slightly into the cytoplasmic periphery (see Fig. 2*C* and supplemental Fig. S1).

Next, we examined the dynamics of B56α-GFP in live HeLa cells by FRAP assay (Fig. 2*D*). Cells were analyzed for a shift in nuclear to cytoplasmic (export) or cytoplasmic to nuclear (import) fluorescence before and after laser bleaching of the cytoplasm or nucleus, respectively. The data showed that B56α comprises both dynamic and poorly mobile pools, and of the actively mobile pool the rate of nuclear export is stronger than import, supporting the predominant cytoplasmic staining observed.

The Sequence Amino Acids 294–486 Is Important for B56α Cytoplasmic Localization—To map the transport elements of B56α, we cloned a series of overlapping B56α sequences as GFP fusions and quantified their subcellular distribution in transfected U2OS cells by fluorescence microscopy. The results are summarized in Fig. 3*A*, and typical cell images are displayed in Fig. 3*B*. The strongest nuclear localization activity was contained within the N-terminal sequence 1–190, which is rich in basic amino acids and accumulated strongly in the nucleus in >60% of cells in the absence of LMB treatment. The B56α sequence amino acids 159–329 displayed a weaker nuclear localization activity. The C-terminal sequence amino acids

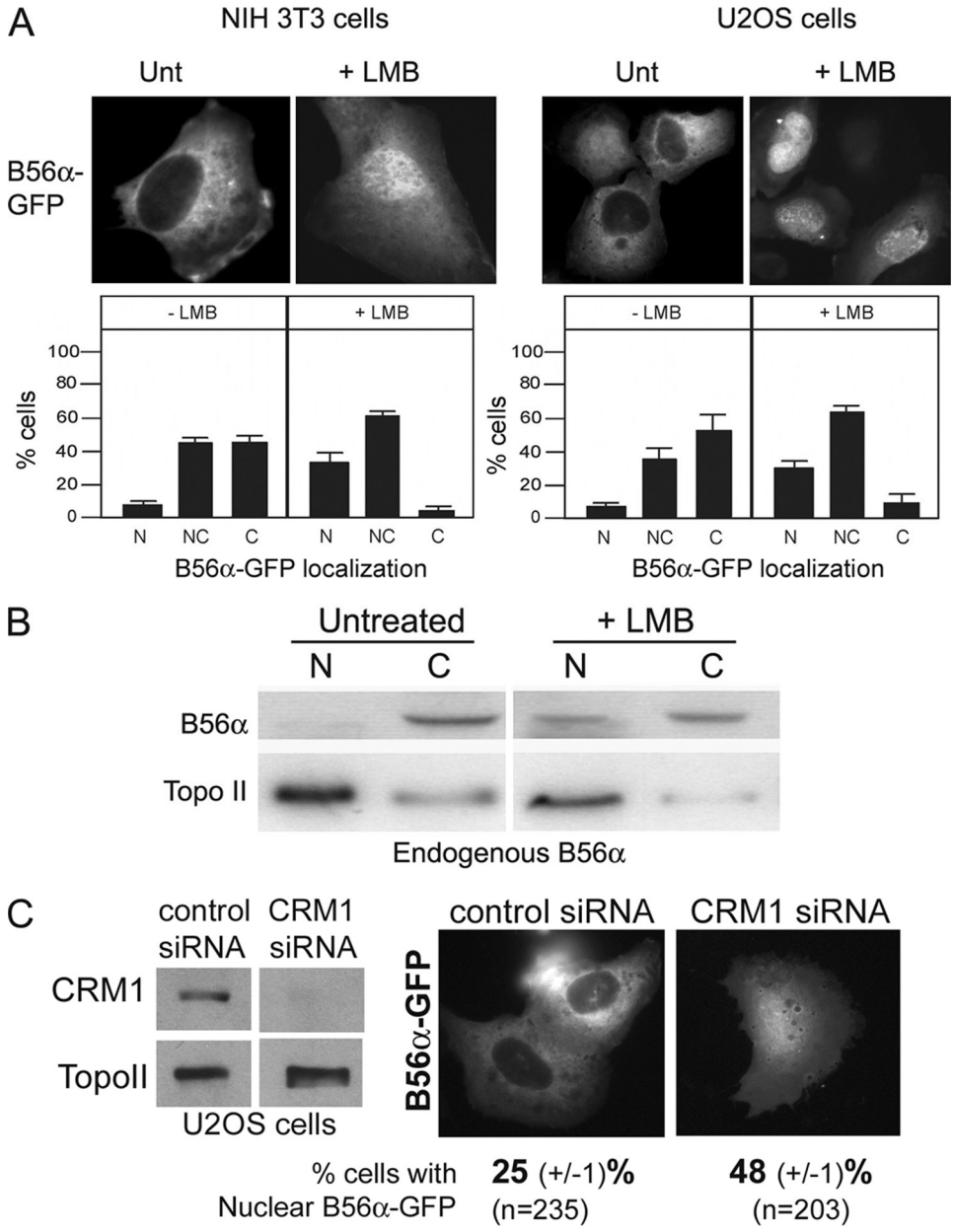

FIGURE 1. **Nuclear-cytoplasmic distribution of B56α is regulated by the CRM1 inhibitor leptomycin B.** *A*, the pB56α-GFP construct was transfected into NIH 3T3 and U2OS cells and nuclear-cytoplasmic distribution was assessed by immunofluorescence microscopy. Typical cell staining patterns are shown, illustrating the nuclear shift induced after a 3-h treatment with LMB. The % cells displaying nuclear (*N*), cytoplasmic (*C*), or nuclear/cytoplasmic (*NC*) staining are graphed as mean and standard deviation. Data shown reflect three experiments scoring at least 100 cells in each experiment. *B*, endogenous B56α distribution was assayed in NIH 3T3 cells by probing Western blots of fractionated cell extracts with antibody against B56α or the nuclear marker Topoisomerase II. LMB treatment shifted B56α to the nucleus. *C*, CRM1 expression was silenced by siRNA in U2OS cells (Western blot, *left panel*) and the effect on nuclear staining of B56α-GFP scored by microscopy (*right panel*). The silencing of CRM1 expression is not as effective as inactivation by LMB, but did cause a reproducible nuclear shift in B56α.

294–486 was predominantly cytoplasmic (though some nucleolar staining was also visible) and did not shift to the nucleus with LMB treatment. This suggested the presence of an NES within amino acids 294–486 if the lack of LMB response was due to absence of a nuclear localization signal. Indeed, the slightly longer sequence amino acids 159–486 did shift to the nucleus after LMB treatment, indicating the presence of both nuclear import and export sequences.

Identification of Conserved Nuclear Export Sequences in B56α, B56β, and B56ϵ—We previously helped define the consensus sequence for active NESs (18), and here identified three potential CRM1-responsive NESs within the C-terminal half of B56α (Fig. 4*A*). These sequences (corresponding to short 13–19 amino acid peptides) were cloned into the pRev(1.4)-GFP vector and tested for their ability to shift an export-defective Rev-GFP reporter protein from the nucleus to the cytoplasm using a transport assay we developed (18). The export assay was performed in T47D cells. Of the three sequences tested, only one displayed nuclear export activity, and it was quite potent and comparable to the positive control NES from HIV REV protein (Fig. 4*B*). In untreated cells the B56α NES (amino acids 451–469) shifted GFP to the cytoplasm, and this was blocked by inhibiting CRM1 with 3 h of LMB treatment.

There are five main PP2A B56 subunits each encoded by different genes. We compared the relative sequence conservation of the B56α NES among the different subunits and found that the key large hydrophobic residues, essential for export function (18), were well conserved in the β- and ϵ-subunits, but not in the δ- and γ-subunits (see Fig. 4*C*). The presence of a potential NES therefore correlates extremely well with the known cytoplasmic localization of the B56-α, -β, and -ϵ subunits (7, 8). We therefore tested the β and ϵ sequences in the nuclear export assay and confirmed that they both displayed nuclear export function, although we note that the β-subunit NES activity was lower than that of the α- and ϵ-subunits (Fig. 4, *B* and *C*).

Identification of Critical Residues in the B56α NES and Evidence That Mutagenesis of a Single Amino Acid Causes Nuclear Retention of Full-length B56α—As mentioned above, the presence and spacing of conserved large hydrophobic amino acid residues such as leucine or isoleucine (*bold font* in Fig. 5*A*) is known to be important for nuclear export function. We confirmed the importance of these specific amino acids by mutating three of the critical leucines to alanine within the B56α NES peptide and tested the effect on export

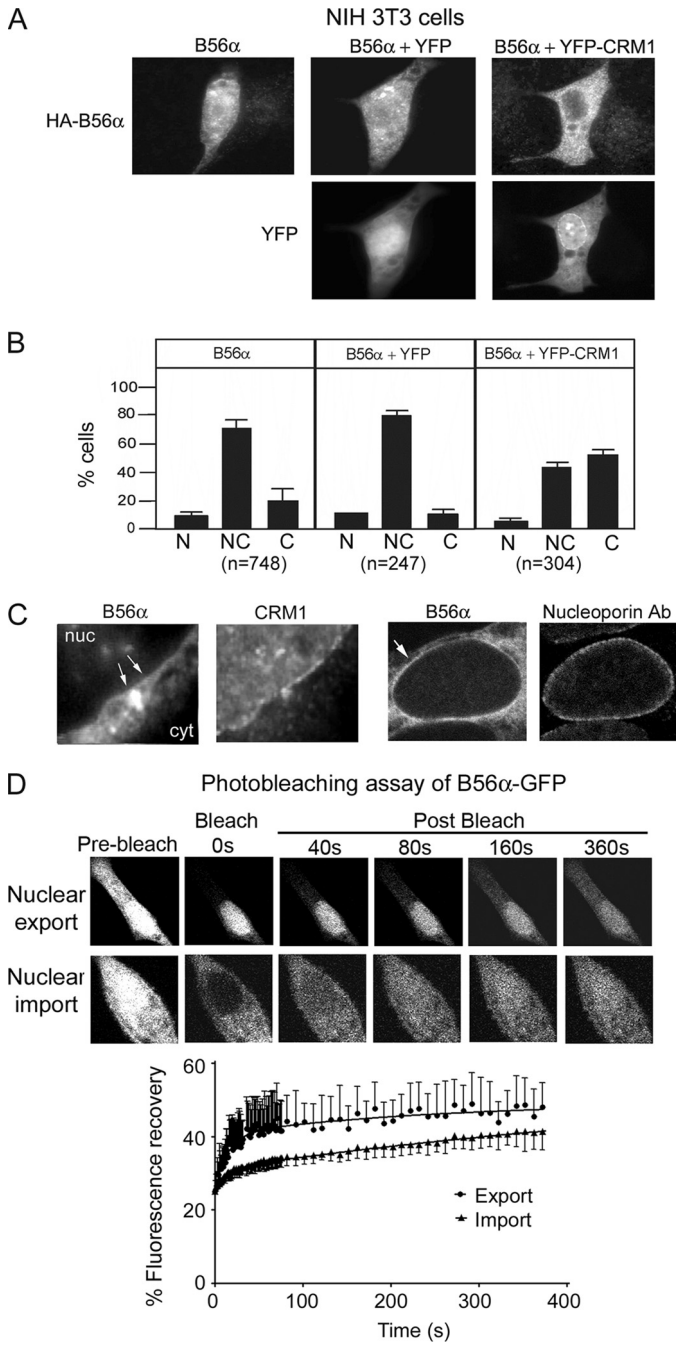

FIGURE 2. **B56α nuclear export is stimulated by overexpression of CRM1 and faster than the rate of import in live cells.** *A*, pHA-B56α was co-transfected into NIH 3T3 cells with pEYFP-C1 or pYFP-CRM1 and scored for nuclear and cytoplasmic distribution (as in Fig. 1) by fluorescence microscopy (B56α was detected by staining with anti-HA antibody). Representative images are shown. *B*, the distribution of ectopic HA-tagged B56α was nuclear/cytoplasmic in ~70% of cells both for untransfected or YFP-expressing cells. The co-expression of YFP-CRM1 shifted B56α to the cytoplasm. *C*, B56α-GFP was transiently expressed and its co-localization with CRM1 at the nuclear envelope determined by co-staining NIH 3T3 cells with antibody to endogenous CRM1 and the nucleoporin FG-repeat monoclonal antibody mAb414. *D*, subconfluent HeLa cells were transfected with B56α-GFP and after 30 h subjected to FRAP analysis (see "Materials and Methods"). To measure nuclear export rate in transfected cells, >90% of the cytoplasm was bleached using 100% laser power and fluorescence recovery monitored over 360 s, as shown in tiled cell images at the *top*. For nuclear import, the nuclear fluorescence was bleached and recovery measured. One example cell showing recovery of nuclear fluorescence is shown. The mean recovery curves for B56α import and export were plotted against time (*graph below*). The fluorescence recovery for nuclear export was calculated as the cytoplasmic to nuclear ratio, which was preset to 100% based on pre-bleach values. Similarly, nuclear import was calculated as the ratio of nuclear to cytoplasmic fluorescence. At least 8 cells were tested for each pathway.

function using the nuclear export assay (18). As shown in Fig. 5*A*, the single alanine substitutions at Leu-458, Leu-461, and Leu-463 each abolished measurable export activity in the transport assay.

We then introduced the L461A mutation into a full-length B56α cDNA by site-directed mutagenesis, and compared its subcellular distribution to wild-type B56α by microscopy. When transfected into NIH 3T3 cells, the L461A mutant exhibited a more frequent nuclear staining pattern than wild-type, and its distribution was comparable to that observed after LMB treatment (Fig. 5*B*, supplemental Fig. S2). Similar results were seen in human SW480 cells (supplemental Fig. S2). The L461A mutation also caused a partial nuclear accumulation of ectopic B56α in cell fractions analyzed by Western blot (supplemental Fig. S3).

B56α Contributes to Nuclear Export of the PP2A Catalytic Subunit—The PP2A C-subunit was recently shown to respond to LMB and undergo CRM1-dependent nuclear export (21). Tsuchiya *et al.* (21) reported a potential NES in the C-subunit although individual sequences were not tested for export function. We investigated the possible role of B56α in regulating C-subunit localization, given that transiently expressed B56α is known to associate with the C-subunit (7). We confirmed that endogenous PP2A C-subunit responded to LMB treatment (supplemental Fig. S4), and then showed that overexpression of YFP-CRM1 shifted the distribution of C-subunit effectively to the cytoplasm, compared with overexpression of YFP alone (Fig. 6). Next, we transiently expressed B56α-GFP and found that it functioned similar to CRM1 and shifted the C-subunit to the cytoplasm. In contrast, the L461A NES mutant form of B56α-GFP did not shift C-subunit to the cytoplasm, but instead slightly increased its nuclear intensity when compared with YFP alone (Fig. 6). LMB treatment of cells also blocked the efficacy of B56α export of the C-subunit (data not shown). We conclude that association with B56α contributes to the cytoplasmic localization of PP2A C-subunit.

B56α Is Recruited to Centrosomes through Sequences That Bind the PP2A A-subunit—PP2A activity has been linked to entry and progression of cells through mitosis, and PP2A was reported to accumulate at centrosomes and the mitotic spindle (22). We used confocal microscopy to determine if B56α displayed a similar distribution, and confirmed that B56α-GFP was clearly visible at centrosomes in ~70% of cells analyzed (Fig. 7*A*). The L461A mutant also located at the centrosome, suggesting that targeting did not depend on the NES or CRM1 (data not shown). We then mapped the sequences required for centrosomal recruitment and observed a correlation between centrosome staining and the sequences that bind the PP2A A-subunit (Fig. 7*B*). Next, we co-stained the B56α-GFP transfected cells for the A-subunit and detected a strong co-localization at the centrosome in most cells (Fig. 7*C*). The PP2A A/C dimer is thought to be anchored at the centrosome by the scaffold protein CG-NAP (22, 23). Our data are consistent with the

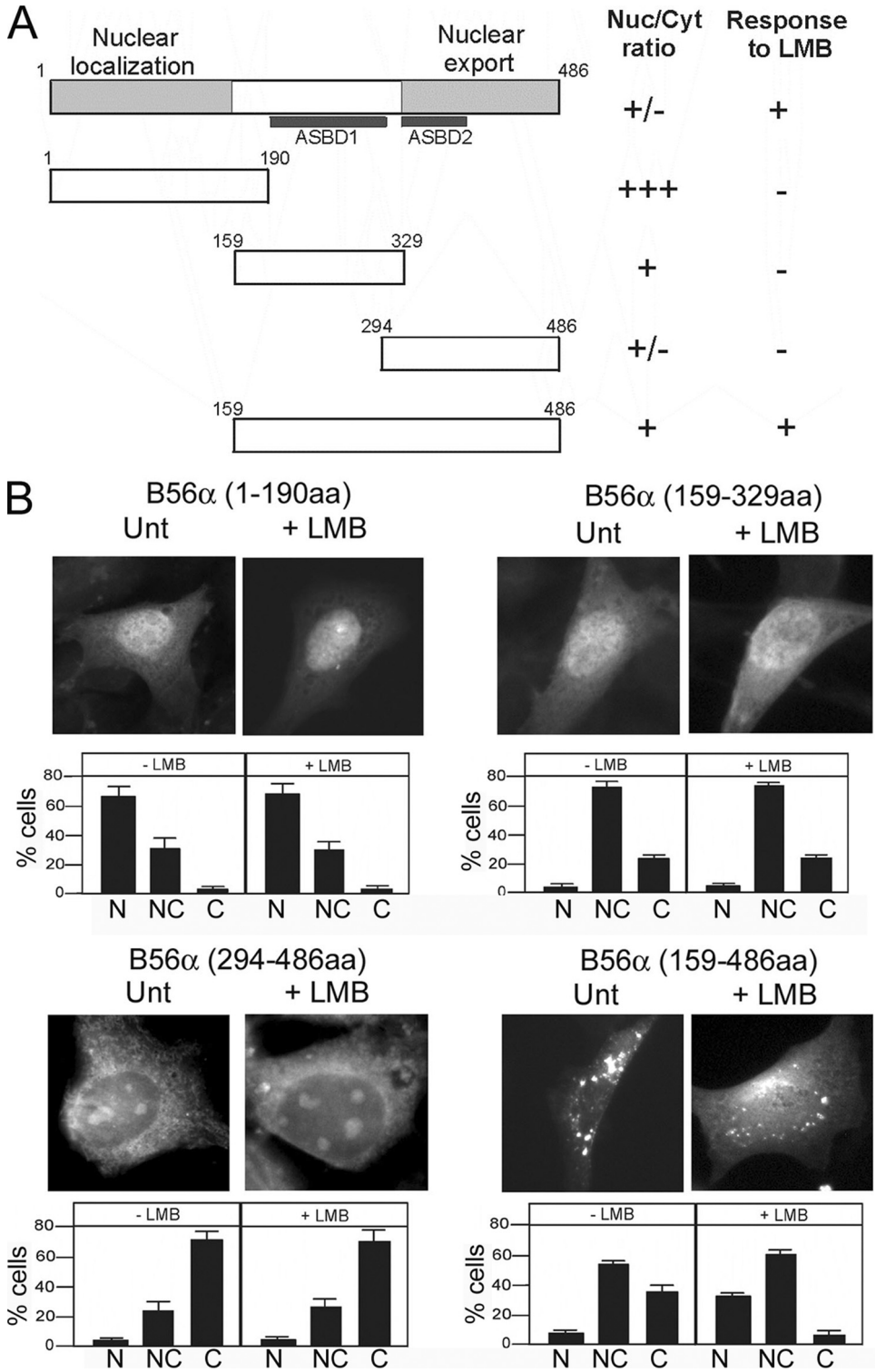

FIGURE 3. **Mapping of export activity to the C terminus of B56α.** *A*, diagram showing the size of overlapping sequences tested for localization and LMB-response after transfection into U2OS cells. The results are summarized at the *right*. The locations of A-subunit binding domains (*ASBD*) are indicated (see Ref. 33). *B*, fluorescence cell images and graphical quantification of the subcellular distribution of B56α (± 3 h LMB) are shown. The data indicate that LMB responsiveness maps to the C-terminal amino acids 294–486.

possibility that the PP2A A-subunit recruits B56α to the centrosome.

Use of Photobleaching Assays to Demonstrate Centrosomal Retention of B56α in Living Cells—The rate of recruitment and degree of retention of B56α-GFP at the centrosome was determined by FRAP assays in live cells using an Olympus FV1000 confocal microscope. The B56α-GFP was detected at the centrosome and after high intensity laser spot-bleaching of centrosome fluorescence we measured recovery at 1-s intervals over a 160-s period (Fig. 8*A*). The correct centrosomal localization was determined by co-expression of the centrosomal marker, RFP-pericentrin, in live cells. The cell images in Fig. 8*A* show two centrosomes of which only one was bleached and the recovery monitored over time. Typical of 8 different cells tested, the fluorescence was bleached to about 28% of the original level and did not significantly recover over the 160-s period. This contrasted with spot-bleaching of other random areas of the cytoplasm which recovered much faster and up to ~75% of pre-bleach levels (Fig. 8*B*). We therefore conclude that B56α does not turn over rapidly at the centrosome, but is stably retained at this structure (up to 70% of the centrosomal pool is immobile), possibly in complex with the PP2A A-subunit.

DISCUSSION

The regulatory B56 subunits of PP2A play important functional roles in different signaling pathways however little attention has been given to their regulation. In this study we addressed the intracellular transport and distribution of the B56α subunit (outlined in Fig. 9), and show that both endogenous and ectopic forms of B56α are predominantly cytoplasmic and shift to the nucleus after inactivation or silencing of the CRM1 export receptor. Consistent with a regulatory role, the nuclear localization and export activities were contained within the N-terminal and C-terminal ends of B56α, respectively, thereby flanking the central PP2A active subunit binding site. We identified a functional NES at the C terminus of B56α and this sequence was required for B56α-mediated nuclear export of the PP2A catalytic subunit. Nuclear export signals were also identified at similar positions in two other B56 subunits known to locate in the cytoplasm. We further detected B56α at the centrosome where

it displayed a slow turnover *in vivo*, indicative of a stable retention and function. Our findings provide new insights into the role of B56α as a PP2A regulator and have implications for a wide-spread role of CRM1-mediated nuclear export in the trafficking of other PP2A B regulatory subunits.

The shuttling of B56α implies a potential activity within the nucleus. Previously, Patturajan *et al.* (13) showed that B56α forms a complex with GSK-3β and the cancer-associated isoform (ΔNp63) of p63 (a p53 homologue). The ΔNp63 protein was found to bind to the N terminus of B56α (amino acids 76–150), and its overexpression caused a nuclear accumulation of B56α in transfected HEK293 cells. In immunoprecipitation assays, B56α bound to GSK-3β and ΔNp63 in the nucleus, leading to the proposal that the overexpression of ΔNp63 seen in cancer cells reduced B56α/PP2A-dependent activation of GSK-3β and subsequently promoted β-catenin stability and nuclear expression which are typically observed in tumor cells. Whereas these claims were speculative, they suggest that ΔNp63 could contribute to the role of the N terminus of B56α in mediating nuclear entry. The striking nuclear accumulation of the B56α N-terminal sequence (1–190) is suggestive of an active NLS (Fig. 3), although it is possible that binding partners such as ΔNp63 also modulate B56α nuclear import or retention. We previously reported that B56α bound to the APC tumor suppressor and enhanced its accumulation in the nucleus (15). Further study is required to better define the nuclear activities and partners of B56α.

Role of B56α as a Nuclear Export Chaperone—Our study expands on the concept that localization of PP2A complexes are regulated by nuclear-cytoplasmic shuttling. This is likely to vary with tissue and cell type due to the large number of predicted trimeric forms of PP2A that can assemble. Previously, only a few studies reported regulation of PP2A subunits by nuclear transport. The first suggested a direct interaction between the active A-subunit and members of the importin-β superfamily, and postulated that the A-subunit itself could regulate the transport process or utilize it to move between nucleus and cytoplasm (24). More recently, Tsuchiya *et al.* (21) reported that the catalytic C-sub-

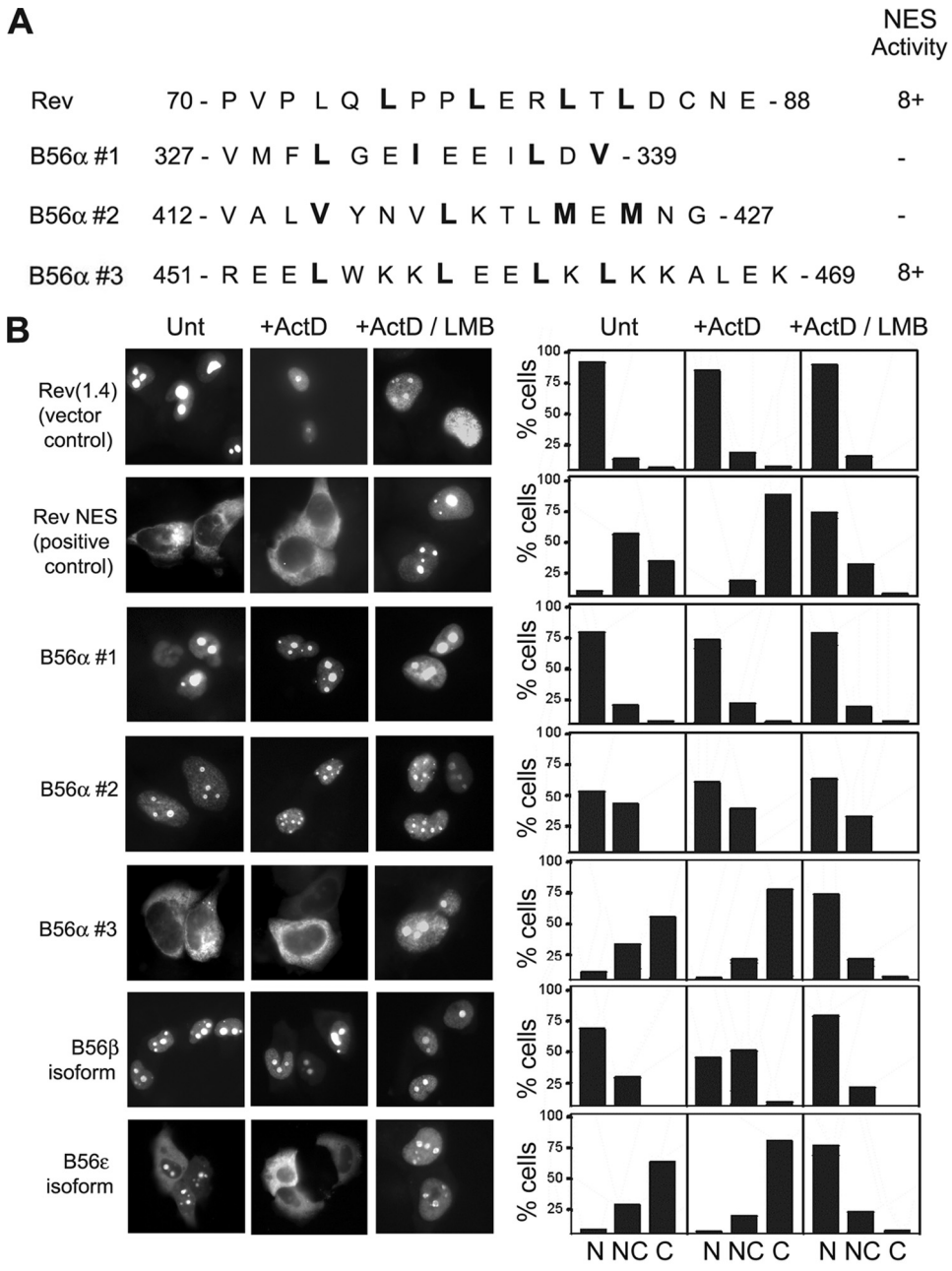

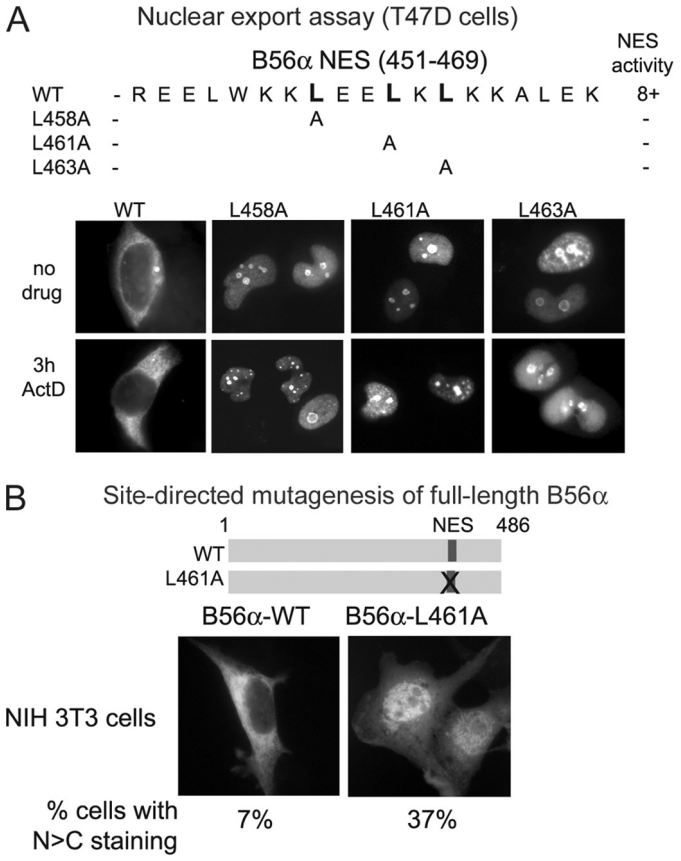

FIGURE 5. **Point mutations in the NES abrogate nuclear export of full-length B56α.** *A*, various mutations were introduced into the NES sequence, converting leucine to alanine at the indicated positions, and cloned into the 1.4-GFP vector to test their effect on nuclear export. Cell images shown are typical of the various B56α NES-GFP fusions following transfection into T47D cells. The relative export activity of these short NES peptides was determined as described under "Materials and Methods." Leucines 458, 461, and 463 were all critical for export activity, and their mutation to alanine prevented export of the GFP reporter. *B*, a single amino acid substitution was next introduced into full-length B56α cDNA to create the NES mutant L461A. Immunofluorescence images are shown of ectopic wild-type and mutated B56α-GFP following transfection into NIH 3T3 cells. The NES mutation caused a nuclear shift in full-length B56α.

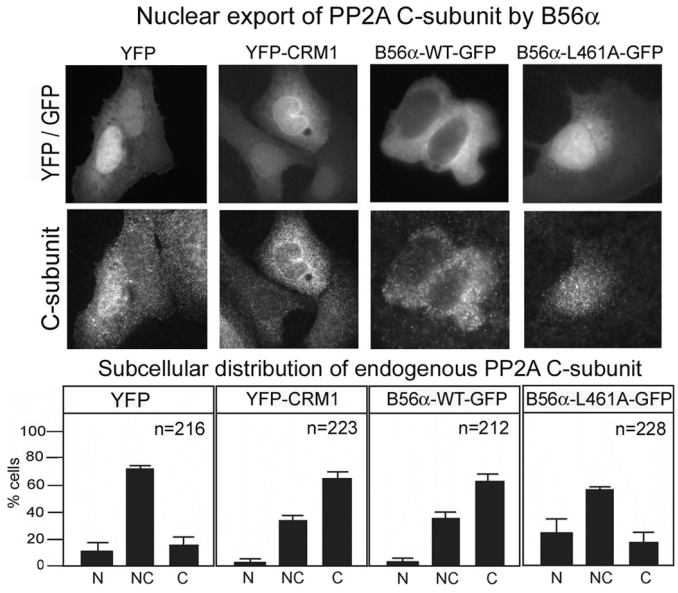

FIGURE 6. **B56α and CRM1 stimulate nuclear export of PP2A catalytic subunit.** U2OS cells were transfected with plasmids expressing YFP, YFP-CRM1, and the GFP-tagged forms of wild-type (*WT*) or NES-mutated (*L461A*) B56α. The cells were then stained for detection of the PP2A C-subunit and analyzed by microscopy. Representative cell images of transfected cells are shown in *top panel*, and below are graphs showing the change in distribution of endogenous PP2A C-subunit following transfection. Overexpression of CRM1 and B56α stimulated nuclear export of C-subunit, and the B56α-dependent export was totally blocked by the L461A mutation.

unit of PP2A accumulated in the nucleus in response to LMB treatment of NIH 3T3 cells after serum arrest. They identified a potential NES in the PP2A C-subunit between amino acids 149 and 158 although the sequence itself was not directly tested for export function. In this study we confirmed the shuttling of endogenous C-subunit and showed that B56α was equally as efficient as CRM1 in effecting nuclear export of the C-subunit (Fig. 6). Importantly, a single amino acid change (L461A) that blocked nuclear export of B56α, also blocked the regulation of C-subunit. These data indicate that B56α is capable of shifting the PP2A C-subunit out of the nucleus.

There is evidence that other B-subunits might also regulate PP2A localization. Jin *et al.* (25) recently identified a nuclear localization activity in the N-terminal 76 amino acids of the B56ϵ subunit, and discovered that a shorter alternatively translated isoform, which lacked the N terminus was more cytoplasmic. They observed an LMB response for B56ϵ and proposed that it contained an undefined nuclear export signal within the region amino acids 76–467 that contributed to cytoplasmic localization. Our discovery of a highly potent NES (amino acids 443–461) at the extreme C terminus of B56ϵ (Fig. 4) helps to clarify that study and explain why the N-terminal truncated form of B56ϵ was more exclusively cytoplasmic than full-length B56ϵ (25). We speculate that cells use alternate splicing and translation as mechanisms to generate different NLS or NES-containing forms of the PP2A B56α, -β, and -ϵ regulatory subunits in different tissues and cell types, thereby creating a regulatable gradient of localized phosphatase activity.

B56α Cytoplasmic and Centrosomal Localization—PP2A phosphatase activity regulates numerous processes including cell cycle progression and apoptosis (2, 3, 26). The apoptotic function of B56α was previously linked to mitochondrial localization (10), however rigorous confocal imaging analysis

FIGURE 4. **Identification of a highly active and conserved nuclear export sequence in B56α.** *A*, sequence comparison of three putative NESs of B56α with the well-characterized NES of HIV-1 Rev. The NES activity was scored from 1+ (low activity) to 9+ (maximum activity) and is summarized at the *right* where 8+ is extremely active. *B*, individual B56α NES#3 and related B56ϵ sequences displayed very strong export activity in a transfection-based nuclear export assay. The respective sequences were cloned into the Rev-GFP fusion vector (*1.4-GFP*), transiently transfected into T47D cells, and the subcellular localization of GFP was determined in the presence or absence of actinomycin D (*ActD*), which retards Rev-GFP nuclear import (18). Where indicated, cells were treated with LMB to abrogate nuclear export via CRM1. The NES-deficient 1.4-GFP construct was used as a negative control (not showing any export activity, set to 0). The Rev NES was a positive control. Graphs represent the mean values of two independent experiments, with a variance not exceeding 15%. *C,* conservation of the B56α export sequence in the B56β and B56ϵ isoforms (for sequence comparison refer to Ref. 32) and its relative activity. The B56 NESs contain a series of large hydrophobic amino acids with a 3:2:1 spacing (*shaded areas*) as previously observed (34). The activity of the different B56 NESs was rated according to Henderson and Eleftheriou (18) and reveal very strong export function for B56α and -ϵ, and a weaker but functional NES in B56β.

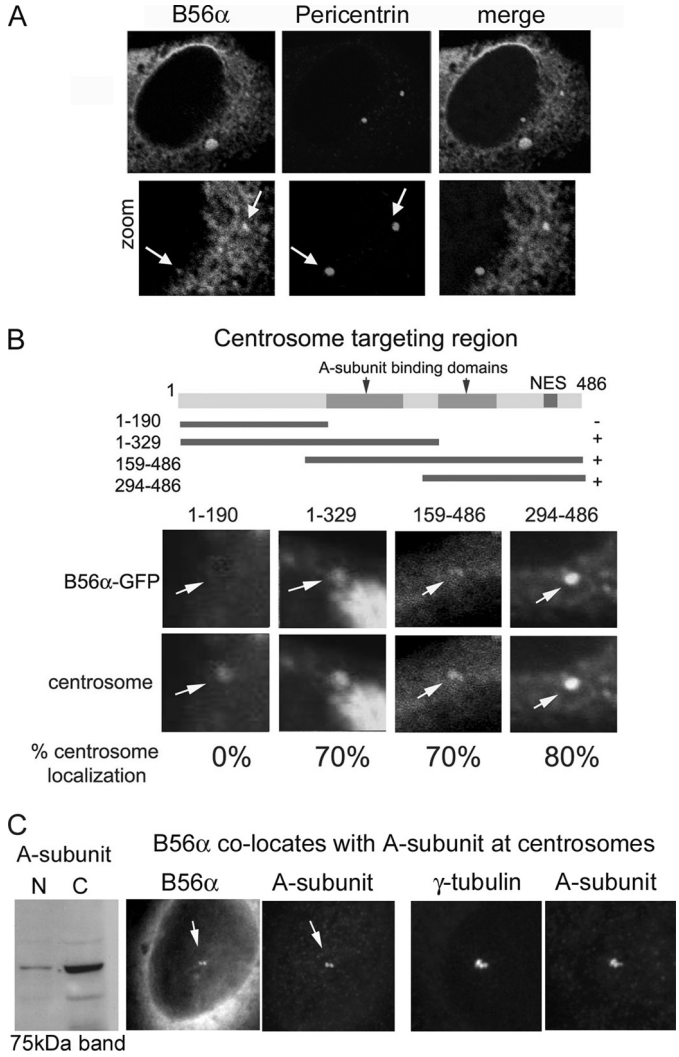

FIGURE 7. **B56α localizes at the centrosome.** *A*, HeLa cells were transfected with B56α-GFP and co-stained with antibody against the centrosomal marker pericentrin (*red*). Confocal microscopy images show co-localization of B56α and the centrosome (see *arrows* in zoom sections). Positive staining was observed in ~70% of cells, as determined by analyzing 25–30 individual cell z-stack images. *B*, to help refine the centrosome targeting region, overlapping B56α sequences were transiently expressed and assessed for centrosome localization as described above. The only sequence that was not detectable at centrosomes was the N-terminal region 1–190. The positive sequences all contain a PP2A A-subunit binding domain, which is known to locate at the centrosome, suggesting that the A-subunit may contribute to anchorage of B56α at centrosomes. *C*, to confirm that B56α-GFP co-localized with the A-subunit at the centrosome, cells were co-stained with antibody against the A-subunit, which displayed strong centrosomal staining (verified by Western and by co-stain with γ-tubulin antibody) in all cells.

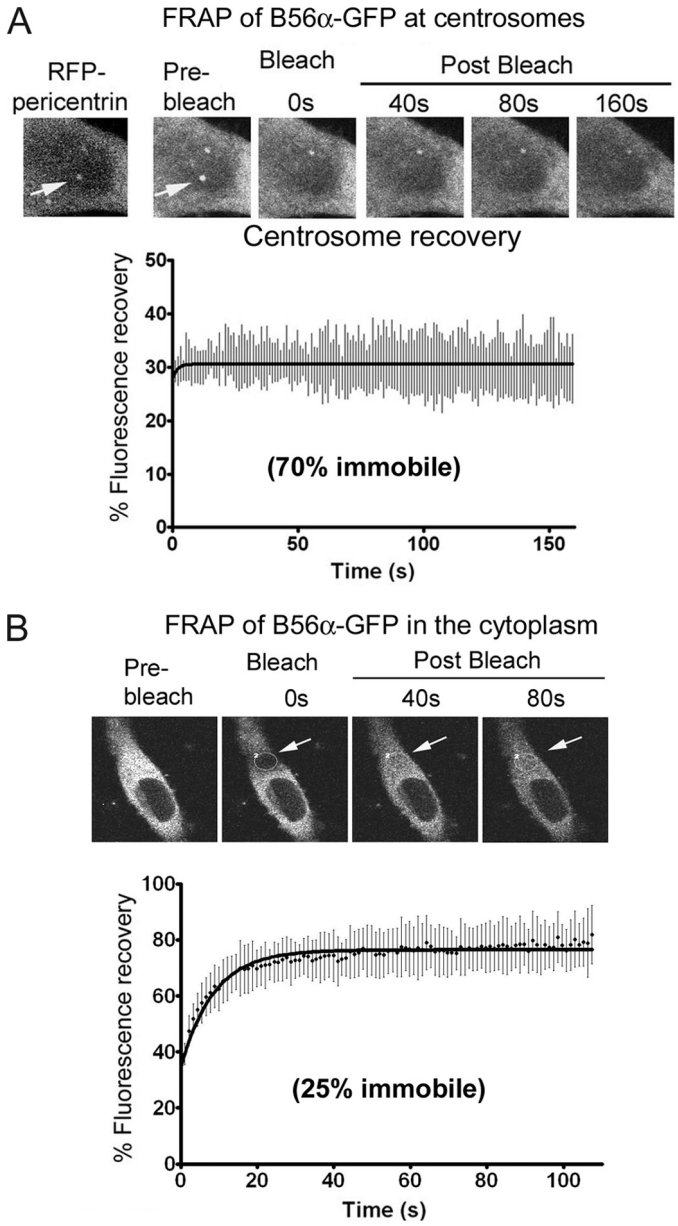

FIGURE 8. **Centrosomal retention of B56α-GFP in live cells measured by FRAP analysis.** *A*, subconfluent HeLa cells were transfected with pB56α-GFP and after 30 h subjected to FRAP analysis with an Olympus FV1000 confocal microscope to measure B56α recruitment to centrosomes in live cells. B56α-GFP fluorescence was detected at the centrosome (Pre-bleach, see *arrow*) and spot-bleached using high-intensity laser (0 s), after which B56α-GFP fluorescence recovery at the centrosome was measured (*top panel* cell images). The centrosomal localization in live cells was marked by co-expression of RFP-pericentrin (a centrosome marker). The tiled images show bleaching of a single centrosome (*arrow*) and poor recovery over a 160-s period. The recovery curve (*below*) reveals almost no recovery of fluorescence intensity after bleaching. Data shown are the average of 8 cells tested. *B*, FRAP analysis of B56α-GFP in the cytoplasm. B56α-GFP was expressed in HeLa cells and spot-bleached with high-intensity laser at random cytoplasmic patches. The fluorescence recovery was then determined at the region of interest and plotted as described above and under "Materials and Methods." Fluorescence recovery was rapid and up to 75% complete within 40 s. Data are from 8 cells analyzed for the recovery curve over a 100-s period.

detected no B56α at the mitochondria (supplemental Fig. S5). The first distinctive cytoplasmic staining we uncovered was at the perinuclear zone, where B56α was observed at the nuclear envelope with some staining extending out into the cytoplasm. It will be interesting to determine if this localization reflects a functional role beyond nuclear transit, such as in nuclear dynamics or nuclear-cytoskeletal positioning.

PP2A activity has also been detected at centrosomes and at the mitotic spindle in mammalian cells (22) and in *Caenorhabditis elegans* (27), with roles in microtubule outgrowth and kinetochore microtubule stability during mitotic spindle assembly (27). In human cells, PP2A subunits are known to associate with cyclin G2 at the centrosome (22). PP2A was found to be anchored stably at centrosomes via binding to the large centrosomal scaffold protein CG-NAP/AKAP450 (23). In this study we detected B56α at the centrosome by confocal microscopy

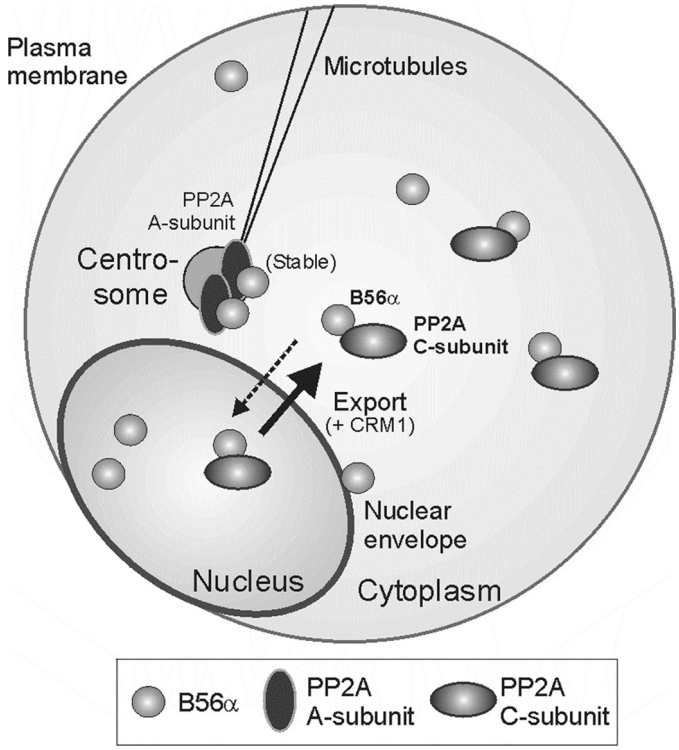

FIGURE 9. **Diagram outlining the subcellular localization of B56α and its role in nuclear export of PP2A catalytic subunit.** This summary outlines the NES-mediated nuclear export of B56α (we predict a similar regulation also for B56-β and B56ϵ subunits which contained active NESs). B56α was detected specifically at the nuclear envelope and at the centrosomes where it co-located with the active subunit. Transient expression of B56α caused a cytoplasmic relocation of the catalytic subunit, and this was dependent on the B56α NES.

(Fig. 7), consistent with previous detection of other PP2A B56 and C-subunits at centrosomes by sucrose gradient fractionation (22). The NES-mutated B56α was also detected at the centrosome, which indicates that targeting is independent of its NES and CRM1. Indeed, the targeting involved sequences that bind to the PP2A A-subunit, and B56α and the endogenous A-subunit were found to co-localize at centrosomes (Fig. 7), suggesting that B56α centrosomal localization is dependent on the PP2A A/C-subunits, rather than the other way round.

The dynamics of B56α were much slower at the centrosome compared with the surrounding cytosol (Fig. 8), indicating that B56α is stably retained at the centrosome and plays an important functional role. This could relate to microtubule growth or centrosome duplication. More specifically, B56α might regulate the β-catenin degradation/phosphorylation complex given that several other Wnt components involved in formation of hyperphosphorylated β-catenin localize to the centrosome. These include Axin (28), APC (29), and phospho-β-catenin itself (30). Alternatively, the centrosomal targeting of B56α could contribute to the role of PP2A in regulating mitosis, an attractive idea supported by recent observations that siRNA knock-down of B56α can induce defects in chromosome segregation in HeLa cells (31).

In conclusion, we identified a CRM1-dependent nuclear export pathway for B56α and showed that this provides a mechanism for regulating nuclear accumulation of the PP2A catalytic subunit. The nuclear export signal peptide we mapped in B56α is not unique, as we identified active NES sequences at similar positions in the related isoforms B56ϵ and B56β, which share strong sequence conservation with B56α (32). Therefore, these findings have general implications for regulation of cytoplasmic and nuclear PP2A phosphatase activity. It is possible that post-translational changes, alternate splicing events or binding to certain proteins could mask the NES and shift B56α to the nucleus. B56α was detected at specific cytoplasmic structures, notably the nuclear envelope/perinuclear zone and the centrosome. We further note that a small number of transfected cells displayed co-localization of B56α with pericentrin at the mid-body during cytokinesis, the final stage of cell separation (see supplemental Fig. S6). The involvement of B56α in PP2A control of mitosis and cytokinesis provides a new functional area for study.

Acknowledgments—We thank other laboratory members for useful discussions and Dr. David Virshup for the B56α plasmid.

REFERENCES

1. Janssens, V., and Goris, J. (2001) *Biochem. J.* **353,** 417–439
2. Eichhorn, P. J., Creyghton, M. P., and Bernards, R. (2009) *Biochim. Biophys. Acta* **1795,** 1–15
3. Virshup, D. M., and Shenolikar, S. (2009) *Mol. Cell* **33,** 537–545
4. Sontag, E., Nunbhakdi-Craig, V., Bloom, G. S., and Mumby, M. C. (1995) *J. Cell Biol.* **128,** 1131–1144
5. Cegielska, A., Shaffer, S., Derua, R., Goris, J., and Virshup, D. M. (1994) *Mol. Cell. Biol.* **14,** 4616–4623
6. Virshup, D. M., Kauffman, M. G., and Kelly, T. J. (1989) *EMBO J.* **8,** 3891–3898
7. McCright, B., Rivers, A. M., Audlin, S., and Virshup, D. M. (1996) *J. Biol. Chem.* **271,** 22081–22089
8. Gigena, M. S., Ito, A., Nojima, H., and Rogers, T. B. (2005) *Am. J. Physiol. Heart Circ. Physiol.* **289,** H285–H294
9. Arnold, H. K., and Sears, R. C. (2006) *Mol. Cell. Biol.* **26,** 2832–2844
10. Ruvolo, P. P., Clark, W., Mumby, M., Gao, F., and May, W. S. (2002) *J. Biol. Chem.* **277,** 22847–22852
11. Seeling, J. M., Miller, J. R., Gil, R., Moon, R. T., White, R., and Virshup, D. M. (1999) *Science* **283,** 2089–2091
12. Li, X., Yost, H. J., Virshup, D. M., and Seeling, J. M. (2001) *EMBO J.* **20,** 4122–4131
13. Patturajan, M., Nomoto, S., Sommer, M., Fomenkov, A., Hibi, K., Zangen, R., Poliak, N., Califano, J., Trink, B., Ratovitski, E., and Sidransky, D. (2002) *Cancer Cell* **1,** 369–379
14. Creyghton, M. P., Roël, G., Eichhorn, P. J., Hijmans, E. M., Maurer, I., Destrée, O., and Bernards, R. (2005) *Genes Dev.* **19,** 376–386
15. Galea, M. A., Eleftheriou, A., and Henderson, B. R. (2001) *J. Biol. Chem.* **276,** 45833–45839
16. Yamamoto, H., Hinoi, T., Michiue, T., Fukui, A., Usui, H., Janssens, V., Van Hoof, C., Goris, J., Asashima, M., and Kikuchi, A. (2001) *J. Biol. Chem.* **276,** 26875–26882
17. Rodríguez, J. A., and Henderson, B. R. (2000) *J. Biol. Chem.* **275,** 38589–38596
18. Henderson, B. R., and Eleftheriou, A. (2000) *Exp. Cell Res.* **256,** 213–224
19. Johnson, M., Sharma, M., Jamieson, C., Henderson, J. M., Mok, M. T., Bendall, L., and Henderson, B. R. (2009) *Cell. Signal.* **21,** 339–348
20. Gillingham, A. K., and Munro, S. (2000) *EMBO Rep.* **1,** 524–529
21. Tsuchiya, A., Tashiro, E., Yoshida, M., and Imoto, M. (2007) *Oncogene* **26,** 1522–1532
22. Arachchige, Don, A. S., Dallapiazza, R. F., Bennin, D. A., Brake, T., Cowan, C. E., and Horne, M. C. (2006) *Exp. Cell Res.* **312,** 4181–4204
23. Takahashi, M., Shibata, H., Shimakawa, M., Miyamoto, M., Mukai, H., and Ono, Y. (1999) *J. Biol. Chem.* **274,** 17267–17274

24. Lubert, E. J., and Sarge, K. D. (2003) *Biochem. Biophys. Res. Comm.* **303,** 908–913
25. Jin, Z., Shi, J., Saraf, A., Mei, W., Zhu, G. Z., Strack, S., and Yang, J. (2009) *J. Biol. Chem.* **284,** 7190–7200
26. Shi, Y. (2009) *Sci. China Ser. C-Life Sci.* **52,** 135–146
27. Schlaitz, A. L., Srayko, M., Dammermann, A., Qunitin, S., Wielsch, N., MacLeod, I., de Robillard, Q., Zinke, A., Yates, J. R., Muller-Reichert, T., Shevchenko, A., Oegema, K., and Hyman, A. A. (2007) *Cell* **128,** 115–127
28. Fumoto, K., Kadono, M., Izumi, N., and Kikuchi, A. (2009) *EMBO Rep.* **10,** 606–613
29. Louie, R. K., Bahmanyar, S., Siemers, K. A., Votin, V., Chang, P., Stearns, T., Nelson, W. J., and Barth, A. I. (2004) *J. Cell Sci.* **117,** 1117–1128
30. Huang, P., Senga, T., and Hamaguchi, M. (2007) *Oncogene* **26,** 4357–4371
31. Cadot, B., Brunetti, M., Coppari, S., Fedeli, S., de Rinaldis, E., Dello Russo, C., Gallinari, P., De Francesco, R., Steinkühler, C., and Filocamo, G. (2009) *Cancer Res.* **69,** 6074–6082
32. McCright, B., and Virshup, D. M. (1995) *J. Biol. Chem.* **270,** 26123–26128
33. Li, X., and Virshup, D. M. (2002) *Eur. J. Biochem.* **269,** 546–552
34. Fabbro, M., and Henderson, B. R. (2003) *Exp. Cell Res.* **282,** 59–69